

# On the nature of large-scale defect accumulations in Czochralski-grown silicon

V P Kalinushkin, A N Buzynin, V A Yuryev, O V Astafiev  
and D I Murin

General Physics Institute of the Russian Academy of Sciences, 38, Vavilov Street,  
Moscow, GSP-1, 117942, Russia

**Abstract.** Czochralski-grown boron-doped silicon crystals were studied by the techniques of the low-angle mid-IR-light scattering and electron-beam-induced current. The large-scale accumulations of electrically-active impurities detected in this material were found to be different in their nature and formation mechanisms from the well-known impurity clouds in a float zone-grown silicon. A classification of the large-scale impurity accumulations in CZ Si:B is made and point centers constituting them are analyzed in this paper. A model of the large-scale impurity accumulations in CZ-grown Si:B is also proposed.

## 1. Introduction

The detection of the large-scale impurity accumulations (LSIAs) with the sizes ranged from several to several tens  $\mu\text{m}$  in CZ Si by means of the low-angle light scatter (LALS) [1] was reported for the first time in Ref. [2]. It was supposed in that work that LSIAs are analogous in their nature to the oxygen and carbon clouds observed in FZ Si in Ref. [3]. It was shown, however, as a result of the research of Si crystals grown at variable growth rate done by LALS and EBIC that most of LSIAs in CZ Si have a shape close to cylindrical [4] which contradict the cloud model [2]. In the present work, an attempt is made to select different in their nature types of LSIAs in CZ Si and an information about their parameters as well as the influence of different thermal treatments on them is given.

## 2. Experimental details

Industrial 76 and 100-mm substrates of CZ Si:B grown in the  $\langle 100 \rangle$  and  $\langle 111 \rangle$  directions —  $\rho \sim \text{several } \Omega\text{cm}$  — were studied in this work. The oxygen concentration in them ranged from  $6 \times 10^{17}$  to  $10^{18} \text{ cm}^{-3}$ , the carbon concentration was less than  $10^{16} \text{ cm}^{-3}$ . The thickness of 76-mm substrates was  $380 \mu\text{m}$ , that of 100-mm ones was  $500 \mu\text{m}$ .

The investigation was carried out by LALS and EBIC. CO- and CO<sub>2</sub>-lasers oscillating at the wavelength of 5.4 and 10.6  $\mu\text{m}$ , respectively, were used in LALS to select

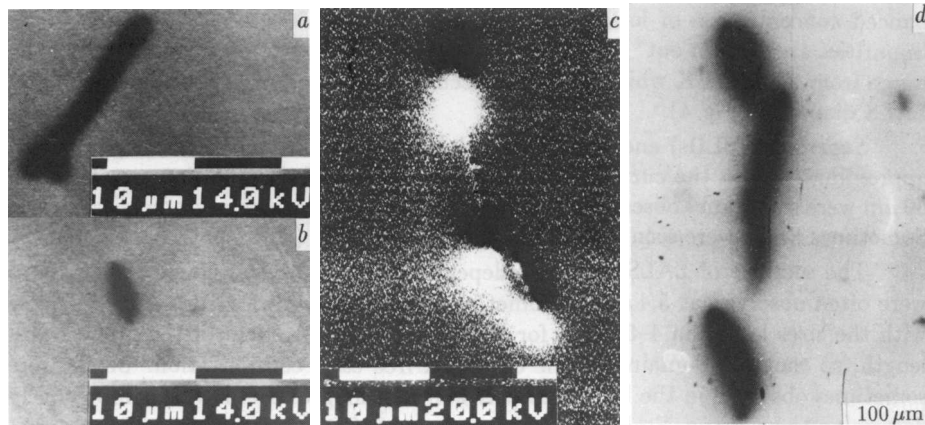


**Figure 1.** EBIC microphotographs of as-grown CZ Si:B: cylindrical (*a*, *b*), spherical (*c*) and superlarge (*d*) defects.

the scattering by free carrier accumulations [5]. To determine the activation energies ( $\Delta E$ ) of the centers constituting LSIAs, the temperature dependences of LALS were investigated in the range from 85 to 300 K [6]. A shape of LSIAs was determined from the dependences of the LALS diagrams on the sample orientation with respect to the detection plane. The plasma etching of the sample surface in a special regime before the Schottky barrier creation greatly increased the sensitivity of EBIC to electrically-active defects in crystals [7].

In the experiments on annealings, wafers were cut into four sections. One of them was not treated, the others were subjected to either isothermal processes at 600 or 800°C for 24, 48 and 120 h, respectively, or high-temperature treatments at 965, 1100, 1150, 1200 and 1250°C for several tens minutes. The treatments at  $T > 1200^\circ\text{C}$  resulted in the formation of a large amount of defects of structure which were revealed by the selective etching (SE). The substrates grown in the  $\langle 100 \rangle$  direction were subjected to both the former and the latter treatments, while those grown in the  $\langle 111 \rangle$  direction were treated only in the latter way.

### 3. Results

#### 3.1. Initial samples

Fig.1 demonstrates the EBIC images of defects. The samples contain many non-uniformities with the sizes from several to several tens  $\mu\text{m}$ —mainly cylindrical. In addition, spherical defects are also seen.

*Cylindrical defects* (CDs). There are sections of LALS diagrams, the shape of which is dependent on the sample orientation to the detection plane (Fig. 2,  $\theta < 4.5^\circ$ ). These sections are well fitted with the curves of scattering by cylinders [1] with the diameters from 3–4 to 8–10  $\mu\text{m}$  and length from 15 to 40  $\mu\text{m}$  depending on a sample. They predominantly oriented along the  $\langle 110 \rangle$  direction. It is seen from the EBIC patterns that CDs have rather elliptical or curved-cylindrical shape (Fig.1 (*a*, *b*)). We assume

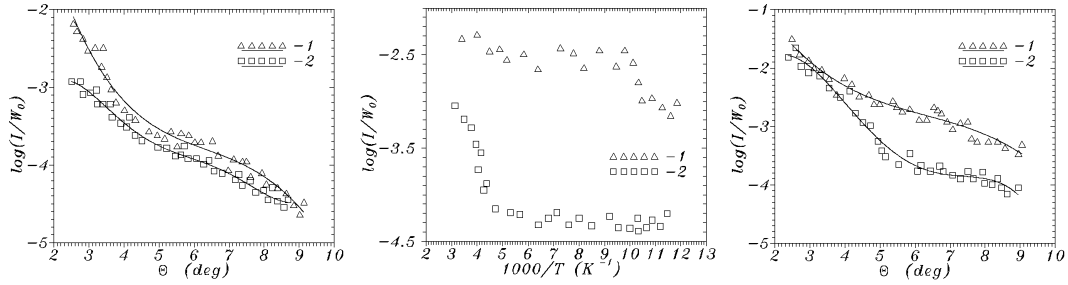


**Figure 2.** LALS diagrams for initial CZ Si:B, orientation with respect to detection plane (deg): 0 (1), 90 (2).

**Figure 3.** LALS temperature dependences for cylindrical (1) and spherical (2) defects in initial CZ Si:B.

**Figure 4.** LALS diagrams at different temperatures (K): 300 (1), 110 (2).

the CDs revealed by EBIC and LALS to be the same defects similar to CDs observed in Ref. [4].

The concentration of CDs—the most usual defects in CZ Si:B—estimated from EBIC ranged from  $10^6$  to  $10^7$   $\text{cm}^{-3}$ . We could not find a dependance of the CD concentration on oxygen concentration, growth direction, ingot diameter or location on a wafer. Nonetheless we found their concentration to vary within a wafer as well as in different wafers.

LALS at 10.6 and 5.4- $\mu\text{m}$  wavelength showed CDs to be domains of the enhanced free carrier concentration [5]. Using the CD concentrations from EBIC, the variations of the dielectric function ( $\Delta\epsilon$ ) and the maximum free carrier concentration in them ( $\Delta n_{\text{max}}$ ) were evaluated [1]: they are  $(1-4) \times 10^{-4}$  and  $(3-10) \times 10^{15} \text{ cm}^{-3}$ , respectively. CDs occupy less than 3 % of crystal volume and the total amount of impurities contained in them ( $N_i$ ) is not greater than  $3 \times 10^{14} \text{ cm}^{-3}$ .

LALS temperature dependences showed for CDs a small (2–3 times) drop of the scattering intensity ( $I_{\text{sc}}$ ) at about 90 K (Fig. 3, curve 1). This allows us to state that LALS by CDs at 300 K at 10.6  $\mu\text{m}$  is controlled by the centers with  $\Delta E \approx 40-60$  meV containing in CDs. Naturally another defects, such as deep or compensating centers as well as precipitates, inclusions and structural imperfections can also be contained in CDs.

*Spherical defects (SDs).* Besides the above sections of LALS diagrams, those independent of the sample orientation were also observed (Fig. 2,  $\theta > 4.5^\circ$ ). These sections are well fitted with the curves of light scattering by spherical defects with the Gaussian profile of  $\epsilon$  [1] and sizes from 5–8 to 20  $\mu\text{m}$ . Such defects are also seen in the EBIC pictures (Fig. 1 (c)). Their concentration is usually about  $10^5 \text{ cm}^{-3}$ ,  $\Delta\epsilon \approx (1-3) \times 10^{-3}$ ,  $\Delta n_{\text{max}} \approx (3-9) \times 10^{16} \text{ cm}^{-3}$  [1]. SDs occupy less than 0.04 % of the crystal volume,  $N_i \lesssim 4 \times 10^{13} \text{ cm}^{-3}$ .

LALS temperature dependences showed SDs, like CDs, to be domains with enhanced concentration of ionized at 300 K impurities with  $\Delta E \approx 120-160$  meV. These

impurities are “frozen out” at about 250 K, so SD-related scattering is smothered in the range from 90 to 250 K which enables the accurate selection of CD-related scattering in LALS diagrams (Fig. 4).

*Superlarge* (SLDs) and *small* (SmDs) defects. The sections of LALS diagrams well approximated with the curves of light scattering by defects with the sizes greater than  $50\text{ }\mu\text{m}$  were sometimes observed. These defects appeared to have an asymmetrical shape. Sometimes SLDs were seen in the EBIC photographs (Fig. 1 (d)).

The sections of LALS diagrams independent of the scattering angle (“plateaux”) were often observed at  $5.4\text{ }\mu\text{m}$  (and sometimes at  $10.6\text{ }\mu\text{m}$ ) which correspond to defects with the sizes less than  $4\text{--}5\text{ }\mu\text{m}$ .  $I_{sc}$  for SmDs was also independent of the probe wavelength, so they are domains with the enhanced free carrier concentration.

SmDs were sometimes observed in the EBIC picture as well. Although we could not unambiguously determine their shape, SmDs seem to be very small CDs and SDs rather than a separate class of defects. This was verified by LALS temperature dependences: SmDs were “frozen out” at 90 K when CDs predominated and at 250 K if SDs predominated.

### 3.2. Annealed samples

The LALS diagrams and EBIC pictures for the annealed crystals did not differ in general features from those for the as-grown samples. The following peculiarities may be emphasized.

1. In crystals annealed in the temperature range of  $600\text{--}1100^\circ\text{C}$ , the light scatter by SDs was greatly (but not completely) suppressed, and CDs and SmDs predominated. EBIC showed mainly CDs and SmDs too.

2. Annealing at  $T > 1100^\circ\text{C}$  resulted in predominance of SD-related scattering and general growth of  $I_{sc}$ . A great number of SDs was observed by EBIC (Fig. 5).

3. After annealing at  $T > 1200^\circ\text{C}$ , the centers with the same  $\Delta E$  as in the as-grown samples composed LSIAs.

4. Annealing at  $800^\circ\text{C}$  and short (up to 48 h) treatment at  $600^\circ\text{C}$  did not change  $\Delta E$  of the centers composing CDs and SDs. Longer treatment at  $600^\circ\text{C}$  resulted in prevailing of the centers with  $\Delta E \approx 70\text{--}90\text{ meV}$  in CDs and SDs.

5. After 120-h annealing at 600 and  $800^\circ\text{C}$ , SLDs became more habitual than in the as-grown samples. The centers with  $\Delta E \approx 130\text{--}170\text{ meV}$  were contained in SLDs.

## 4. Discussion

It is difficult now to determine the nature of LSIAs in CZ Si:B unambiguously. It is clear, however, that CDs are domains with the enhanced free carrier concentration caused by point centers with  $\Delta E \approx 40\text{--}60\text{ meV}$ . CDs look like the defects observed by EBIC after oxidizing annealings [8]. Our research gave an evidence to the presence of these defects in initial crystals, moreover the CD-related sections of LALS diagrams

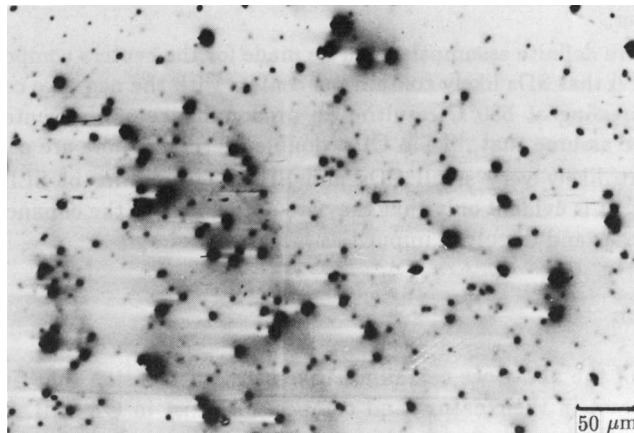


**Figure 5.** Typical EBIC microphotograph of defects in CZ Si:B annealed at  $T > 1100^\circ\text{C}$ .

do not change after high-temperature annealings. In our opinion, however, CDs are the impurity atmospheres (IAs) around defects-precursors, e.g. stacking faults (SFs). Remark that some authors connect the contrast of EBIC patterns with the formation of precipitate colonies around SFs [8]. As these colonies may have no influence on the free carrier concentration in IAs, the following scenario might be proposed.

In initial wafers, the precipitate concentration in IAs is low. At the same time, the dissolved ionized impurity concentration is high enough but insufficient for the precipitate formation, hence  $I_{sc}$  is high and the recombination contrast in EBIC is low. During high-temperature annealing, precipitate colonies arise in CDs but the dissolved impurity concentration and  $\Delta n$  change weakly (e.g. because the impurity concentration in CDs in the as-grown samples was close to the saturation limit or due to the growth of the compensation degree). The recombination contrast will have grown and  $I_{sc}$  will have changed weakly and randomly.

From the other hand, the enhanced EBIC contrast may be caused by the specificity of the sample preparation. Two variants are possible. The centers enhancing the EBIC contrast may arise as a result of the plasma etching applied. Alternatively, an “exhaustion” of CDs may be a result of the chemical etching usually applied for sample preparation for EBIC.

Thus, the hypothesis according to which CDs are IAs around SFs does not meet contradictions. As to the point defects composing CDs, we suppose them to be the “new” thermal donors [9] whose  $\Delta E$  is close to the estimates made<sup>‡</sup>. The influence of  $600^\circ\text{C}$  annealing on  $\Delta E$  of the centers composing CDs indirectly verifies the assumption<sup>§</sup>. New experiments are required to obtain more evidences to the model proposed, though.

SDs also are domains with the enhanced dissolved impurity and free carrier concentrations. We assume SDs to be IAs around defects of structure (e.g. precipitates).

<sup>‡</sup> Although, some alternatives exist [10], and B and [Cu–O] are among them.

<sup>§</sup> The growth of ionization energy of “new” thermal donors as a result of long-term annealing at  $650^\circ\text{C}$  was reported in [11].

This hypothesis is confirmed by the growth of the SD concentration during the high-temperature annealings and correlation with the appearance of structural defects revealed by SE. This assumption also have no sufficient evidences<sup>||</sup> and require an additional research, however.

Some more definite assumption can be made for the centers composing SDs. It was supposed in [12] that SDs likely contain the centers with the negative correlation energy. Regarding annealing at 600°C resulting in predominance of the centers with changed  $\Delta E$  in SDs, we assume that, like in CDs, double thermal donors are contained in SDs<sup>¶</sup>.

SmDs are likely very small CDs and SDs. The nature of SLDs is hard to be discussed now. It is evident only that they are domains with the enhanced concentration of the free carrier and dissolved impurities.

## 5. Conclusion

On the basis of the above we can summarize in the conclusion that at least two types of LSIAs different in their nature and composition exist in CZ Si:B. Their parameters determined for the investigated in this work group of crystals are rather typical for the industrial Si:B with the specific resistivity of several  $\Omega$  cm. Some additional details of this research can be found in Ref. [10].

- [1] Voronkov V V, Voronkova G I, Zubov B V *et al* 1981 *Sov. Phys.–Solid State* **23** (1) 65–75  
Kalinushkin V P 1988 *Proc. Inst. Gen. Phys. Acad. Sci. USSR* vol 4 (New York: Nova) pp 1–79
- [2] Voronkov V V, Voronkova G I, Murina T M *et al* 1983 *Sov. Phys.–Semicond.* **17** (12) 2137–42
- [3] Voronkov V V, Voronkova G I, Zubov B V *et al* 1979 *Sov. Phys.–Semicond.* **13** (5) 846–54
- [4] Buzynin A N, Zabolotskiy S E, Kalinushkin V P *et al* 1990 *Sov. Phys.–Semicond.* **24** (2) 264–70
- [5] Kalinushkin V P, Masychev V I, Murina T M *et al* 1986 *Journ. Tech. Phys. Letters* **12** (3) 129–33
- [6] Zabolotskiy S E, Kalinushkin V P, Murin D I *et al* 1987 *Sov. Phys.–Semicond.* **21** (8) 1364–8
- [7] Buzynin A N, Butylkina N A, Lukyanov A E *et al* 1988 *Bul. Acad. Sci. USSR. Phys. Ser.* **52** (7) 1387–90
- [8] Schmalz K, Kirscht F-G, Niese S *et al* 1985 *Phys. Status Solidi* (a) **89** 389–95
- [9] Bouret A 1985 *Proc. 13 Int. Conf. on Defects in Semiconductors* ed L C Kimerling 129–34
- [10] Astafiev O V, Buzunin A N, Buvaltsev A I *et al* 1994 *Sov. Phys.–Semicond.* **28** (3) 407–15
- [11] Kanamori A and Manamori M 1979 *J. Appl. Phys.* **50** 80–6
- [12] Valiev K A, Velikov L B, Kalinushkin V P *et al* 1990 *Sov. Phys.–Microelectronics* **19** (5) 453–9  
Abdurahimov D E, Bochikashvily P M, Vereschagin V L *et al* 1992 *Microelectronics* **21** (1) 21–7

<sup>||</sup> Some alternatives to the assumption—the cloud models—are discussed in [10].

<sup>¶</sup> Possible alternatives to these centers are discussed in [10], they are  $B_i$ ,  $[O-V]$ ,  $[C_i-C_s]$ , *etc.*